

See discussions, stats, and author profiles for this publication at: <https://www.researchgate.net/publication/235679088>

# Molecular Dynamics Simulation Study of the Capacitive Performance of a Binary Mixture of Ionic Liquids near an Onion-like Carbon Electrode

DATASET · AUGUST 2012

CITATIONS

5

READS

61

7 AUTHORS, INCLUDING:



**Guang Feng**

Huazhong University of Science and Technol...

47 PUBLICATIONS 797 CITATIONS

SEE PROFILE



**Pasquale F Fulvio**

University of Puerto Rico at Rio Piedras

71 PUBLICATIONS 2,254 CITATIONS

SEE PROFILE



**Chen Liao**

Argonne National Laboratory

43 PUBLICATIONS 298 CITATIONS

SEE PROFILE



**Peter T Cummings**

Vanderbilt University

518 PUBLICATIONS 11,688 CITATIONS

SEE PROFILE

# Molecular Dynamics Simulation Study of the Capacitive Performance of a Binary Mixture of Ionic Liquids near an Onion-like Carbon Electrode

Song Li,<sup>†</sup> Guang Feng,<sup>†</sup> Pasquale F. Fulvio,<sup>‡</sup> Patrick, C. Hillesheim,<sup>‡</sup> Chen Liao,<sup>‡</sup> Sheng Dai,<sup>‡,§</sup> and Peter T. Cummings<sup>\*,†,||</sup>

<sup>†</sup>Department of Chemical and Biomolecular Engineering, Vanderbilt University, Nashville, Tennessee 37235, United States

<sup>‡</sup>Chemical Sciences Division, Oak Ridge National Laboratory, Oak Ridge, Tennessee 37831, United States

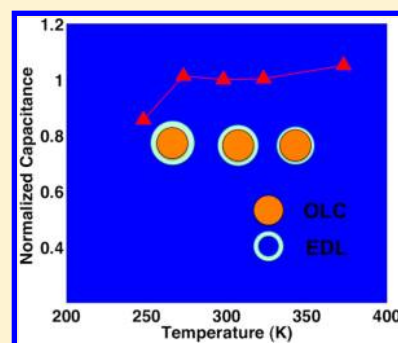
<sup>§</sup>Department of Chemistry, University of Tennessee, Knoxville, Tennessee 37996, United States

<sup>||</sup>Center for Nanophase Materials Science, Oak Ridge National Laboratory, Oak Ridge, Tennessee 37831, United States

## Supporting Information

**ABSTRACT:** An equimolar mixture of 1-methyl-1-propylpyrrolidinium bis-(trifluoromethylsulfonyl)imide ([C<sub>3</sub>mpy][Tf<sub>2</sub>N]), 1-methyl-1-butylpiperidinium bis-(trifluoromethylsulfonyl)imide ([C<sub>4</sub>mpip][Tf<sub>2</sub>N]) was investigated by classic molecular dynamics (MD) simulation. Differential scanning calorimetry (DSC) measurements verified that the binary mixture exhibited lower glass transition temperature than either of the pure room-temperature ionic liquids (RTILs). Moreover, the binary mixture gave rise to higher conductivity than the neat RTILs at lower temperature range. In order to study its capacitive performance in supercapacitors, simulations were performed of the mixture, and the neat RTILs used as electrolytes near an onion-like carbon (OLC) electrode at varying temperatures. The differential capacitance exhibited independence of the electrical potential applied for three electrolytes, which is in agreement with previous work on OLC electrodes in a different RTILs. Positive temperature dependence of the differential capacitance was observed, and it was dominated by the electrical double layer (EDL) thickness, which is for the first time substantiated in MD simulation.

**SECTION:** Energy Conversion and Storage; Energy and Charge Transport



Room-temperature ionic liquids (RTILs) are promising electrolytes in energy storage devices. The application of RTILs in electrical double layer capacitors (EDLCs, also named supercapacitors) that store electric energy in the form of electrical double layer (EDL), has attracted increasing research interest due to its longer cycle life, higher power density and faster charging/discharging rates than organic or aqueous electrolytes.<sup>1–4</sup> The current utility of RTILs is restricted by the limited operating temperature range, which is mostly within 293–353 K. In order for supercapacitors to be used under severe cold weather conditions (specifically, temperatures as low as –50 °C, corresponding to the lower limit for automotive applications), ionic liquids with lower melting points are essential while retaining the capacitance. In this direction, binary mixtures of RTILs exhibited reduced melting temperature than either of the neat RTILs and widened liquidus range,<sup>5</sup> thus favoring the low-temperature application of RTILs. These mixed RTILs with decreased melting points are also referred to as eutectic ionic liquids, since the concentrations chosen correspond to eutectic points on the phase diagram.

To achieve better electrochemical performance, electrolytes consisting of mixed RTILs have been used in lithium batteries<sup>6</sup> and dye-sensitized solar cells.<sup>7</sup> A recent study found that an equimolar mixture of piperidinium- and pyrrolidinium-based

RTILs with the same anion bis(fluorosulfonyl)imide (FSI) as electrolytes near an exohedral onion-like carbon (OLC) electrode exhibited a broadened operation temperature range and increased conductivity at low temperature.<sup>8</sup> Because of the implications of such eutectic mixtures for energy storage and conversion devices, understanding the molecular behavior near electrode surfaces with well-defined surface curvatures is of great importance for further progresses in this field. Hence, it is scientifically interesting to understand the influence of temperature on the capacitive behavior of binary mixtures near the OLC electrode surface. Such electrodes have a simpler surface geometry than most porous carbons normally used as electrodes in supercapacitors. The nonporous OLC electrodes can be described as nearly spherical particles having a concentric fullerene shell structure and exhibiting a narrow particle size distribution. Thus, the simpler exohedral model describing the surfaces of OLCs offers a suitable reference for investigating the positive temperature issues associated with the eutectic mixtures of RTILs on carbon electrodes issue using

Received: July 12, 2012

Accepted: August 20, 2012

molecular dynamics (MD) simulation. In addition, the OLC electrode has been reported as an excellent electrode material owing to high charging rate and power density.<sup>9–11</sup> Such electrodes possess a unique parallel differential capacitance–potential ( $C$ – $V$ ) curve rather than the common bell-, camel- or concave-shaped curves.<sup>12</sup> This property greatly favors the stable performance of supercapacitors.

To date, the influence of temperature on the differential capacitance using RTIL electrolyte has been investigated both experimentally<sup>13–16</sup> and by computational<sup>17–21</sup> methods. Most of the experimental work<sup>13–16</sup> shows that the capacitance increases as temperature increases (positive temperature dependence), a trend also observed in high-temperature molten salts.<sup>22,23</sup> However, the opposite trend (negative temperature dependence) was found for RTILs at a mercury electrode<sup>24</sup> and molten salts at liquid magnesium electrodes.<sup>25</sup> By contrast, theoretical studies have predicted negative temperature dependence for graphite electrodes in MD simulation<sup>17</sup> and RTILs near metal electrodes in Monte Carlo (MC) simulation of the restricted primitive model,<sup>26</sup> while MC simulations,<sup>18</sup> density function theory (DFT),<sup>20</sup> and modified mean spherical approximation (MSA) theory<sup>27</sup> predict bell-shaped temperature dependence. So far, a widely acceptable explanation for these phenomena has not been proposed.

Hence, in this work, atomistic MD simulation, as previously reported for supercapacitors using RTIL electrolytes on flat graphite, and metallic electrode surfaces,<sup>17,28,29</sup> was applied here to model pure and mixed RTILs as electrolytes near an OLC electrode as a function of temperature. The ionic liquid electrolytes used in this study are  $[\text{C}_3\text{mpy}][\text{Tf}_2\text{N}]$ ,  $[\text{C}_4\text{mpip}][\text{Tf}_2\text{N}]$ , and the equimolar mixture of these two ionic liquids. The detailed simulation setup is provided in the Supporting Information (SI). The aim of this work is to interpret how the binary electrolytes at varying temperatures influence the EDL microstructure and the differential capacitance of OLC-based supercapacitors. The results also demonstrate that binary RTIL electrolytes exhibit higher conductivity than either of the neat RTILs; the  $C$ – $V$  curve of the binary mixture near the OLC manifested a shape similar to those of neat RTILs and the differential capacitance values increase as temperature increases; the temperature dependence of capacitance is related to the EDL microstructure, mainly dominated by the EDL thickness.

The typical property of a eutectic mixture is the lowering of the melting ( $T_m$ ) and glass transition temperature ( $T_g$ ) in contrast to those of its individual components. The eutectic property of the 1:1 (by molar ratio) mixture of  $[\text{C}_3\text{mpy}][\text{Tf}_2\text{N}]$  and  $[\text{C}_4\text{mpip}][\text{Tf}_2\text{N}]$  was first examined by differential scanning calorimetry (DSC) (Figure S1 in the SI). The glass transition temperatures for  $[\text{C}_3\text{mpy}][\text{Tf}_2\text{N}]$  and  $[\text{C}_4\text{mpip}][\text{Tf}_2\text{N}]$  were approximately 276 and 197 K, respectively. By contrast, the mixture exhibited a  $T_g$  of 190 K, slightly lower than the  $T_g$  of  $[\text{C}_4\text{mpip}][\text{Tf}_2\text{N}]$ . This result suggests that the binary mixture may solidify at a lower temperature than either pure RTIL, thus suggesting that the mixture will exhibit higher diffusion and ionic conductivity in the same low-temperature region as the pure fluids. The conductivity for the pure and mixed RTILs obtained from both experiment and MD simulation is shown in Figure 1.

Due to experimental limitations for conductivity measurements, the temperature range for conductivity measurements was between 300 and 360 K. In MD simulation, the conductivity was estimated using the Nernst–Einstein approximation (see SI). The highest temperature applied was 373 K,

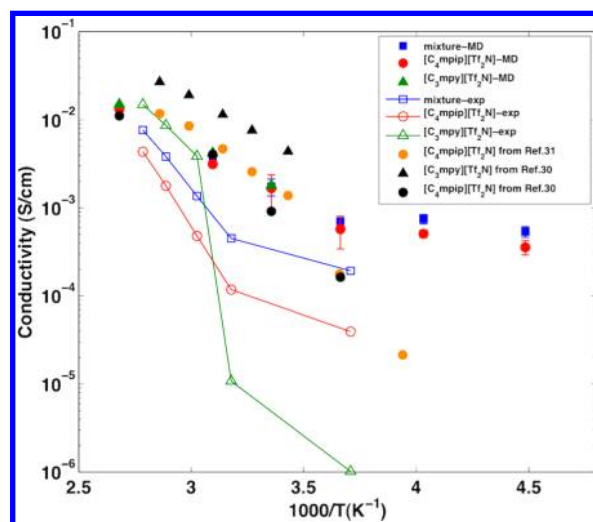


**Figure 1.** Conductivity obtained from experiment and MD simulation as a function of temperature for  $[\text{C}_3\text{mpy}][\text{Tf}_2\text{N}]$ ,  $[\text{C}_4\text{mpip}][\text{Tf}_2\text{N}]$ , and their binary 1:1 mixture.

and the lowest temperature taken herein for each type of RTIL was above their  $T_g$ . For both experiment and MD, it is seen that the conductivity decreases as temperature decreases. At a high temperature range,  $[\text{C}_3\text{mpy}][\text{Tf}_2\text{N}]$  exhibited higher conductivity than  $[\text{C}_4\text{mpip}][\text{Tf}_2\text{N}]$  and the equimolar mixture. As temperature decreases, the conductivity of  $[\text{C}_3\text{mpy}][\text{Tf}_2\text{N}]$  is dramatically reduced by 2–3 orders of magnitude (Figure 1). However, a less pronounced decrease in conductivity for  $[\text{C}_4\text{mpip}][\text{Tf}_2\text{N}]$  and the binary mixture in the high temperature range was observed from both experiment and MD results. Due to the lower  $T_g$ ,  $[\text{C}_4\text{mpip}][\text{Tf}_2\text{N}]$  and the binary mixture remain in the liquid state at lower temperatures, thus exhibiting much higher conductivity than  $[\text{C}_3\text{mpy}][\text{Tf}_2\text{N}]$ . As the temperature decreased to 273 K in the MD simulation, a more significant discrepancy between the conductivities of the binary mixture and that of  $[\text{C}_4\text{mpip}][\text{Tf}_2\text{N}]$  was observed, with the highest conductivities found for the former. Both MD and experiment point to the use of the binary mixture as a low-temperature electrolyte. According to Simon et al.,<sup>8</sup> the binary mixture of RTILs exhibited approximately 5–7 orders of magnitude higher conductivity compared to neat RTILs at low temperature ranges. In this study, at the lowest temperature of 223 K, the conductivity of the binary mixture is approximately 1.5 times of that of  $[\text{C}_4\text{mpip}][\text{Tf}_2\text{N}]$ . Additionally, while previous experimental conductivity measurements<sup>30,31</sup> showed a decrease of several orders for  $[\text{C}_4\text{mpip}][\text{Tf}_2\text{N}]$  as the temperature declined from 373 to 250 K, our MD results exhibited only several times of magnitude reduction. These differences indicated that at high temperature, the simulation correctly predicts the conductivity, both qualitatively and quantitatively; at lower temperature, the simulation does not accurately estimate the quantitative changes, which likely reflect limitations of the force field at low temperatures.

The differential capacitances ( $C_{\text{diff}}$ ) for  $[\text{C}_3\text{mpy}][\text{Tf}_2\text{N}]$ ,  $[\text{C}_4\text{mpip}][\text{Tf}_2\text{N}]$ , and their equimolar mixture were calculated, respectively. Their surface charge densities as a function of potential drop at 373 K are shown in Figure 2a. These exhibit a linear-like relationship with the potential drop for neat and mixed RTILs, indicating that their differential capacitances were equal throughout the potential according to the definition  $C_{\text{diff}} = (d\sigma)/(d\phi_{\text{EDL}})$  ( $\sigma$  is the surface charge density of the electrode;

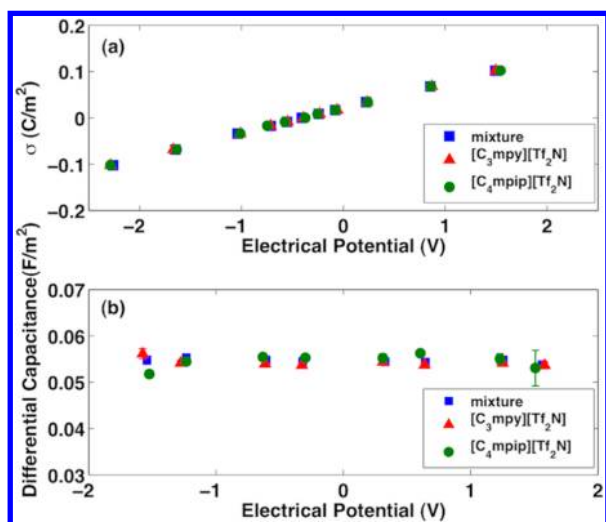


**Figure 2.** (a) Surface charge density as a function of electrical potential drop for  $[C_3\text{mpy}][\text{Tf}_2\text{N}]$ ,  $[C_4\text{mpip}][\text{Tf}_2\text{N}]$ , and their equimolar binary mixture at 373 K. (b) The differential capacitance as a function of electrical potential for  $[C_3\text{mpy}][\text{Tf}_2\text{N}]$ ,  $[C_4\text{mpip}][\text{Tf}_2\text{N}]$ , and their equimolar binary mixture at 373 K.

$\phi_{\text{EDL}}$  is the potential drop across the EDL). Moreover, regardless of the potential applied, the differential capacitances were  $\sim 0.054 \text{ F/m}^2$ . The differential capacitance for all investigated samples, shown in Figure 2b, further suggests that the differential capacitance was identical for both neat and mixed RTILs and is independent of the potential applied. A potential-independent differential capacitance was also observed for 1-ethyl-3-methylimidazolium bis-(trifluoromethylsulfonyl)imide ( $[\text{emim}][\text{Tf}_2\text{N}]$ ) near the OLC electrode.<sup>12</sup> Our results demonstrate that this is also applicable to piperidinium-based RTILs, pyrrolidinium-based RTILs, as well as their binary mixture. This phenomenon has been explained by the dominant role of the charging overscreening at curved electrode surface as the applied potential varies.<sup>12</sup> Recently, Yan et al. proposed that specific adsorption led to the discrepancy of differential capacitance at positively and negatively charged electrodes, which indicates that the lack of specific adsorption may be another cause of potential independent differential capacitance.<sup>32</sup> In the present study,  $[C_3\text{mpy}][\text{Tf}_2\text{N}]$  and  $[C_4\text{mpip}][\text{Tf}_2\text{N}]$  exhibited equivalent differential capacitance, revealing similar EDL structure near OLC. Furthermore, Figure S2 shows the number density profile for three types of electrolytes at 373 K near neutral and charged OLC.  $[C_3\text{mpy}^+]$  is approximately 10% smaller than  $[C_4\text{mpip}^+]$  in size, therefore, the number density in EDL of  $[C_3\text{mpy}][\text{Tf}_2\text{N}]$  is slightly higher than that of  $[C_4\text{mpip}][\text{Tf}_2\text{N}]$ . However, owing to the small differences in molecular weight and size between  $[C_3\text{mpy}][\text{Tf}_2\text{N}]$  and  $[C_4\text{mpip}][\text{Tf}_2\text{N}]$ , their EDLs are very similar, resulting in similar EDL structure for their equimolar mixture.

To achieve extension of the operating temperature range for supercapacitors, the influence of temperature on the performance of supercapacitors requires in-depth investigation. In Figure 3a, a linear dependence of the surface charge density for the binary mixture as a function of the potential applied is presented at the temperatures of 248, 298, and 373 K, respectively. The differential capacitance, obtained from the slope of the linear fitting, increases with increasing temperature (i.e.,  $0.044 \text{ F/m}^2$  at 248 K,  $0.051 \text{ F/m}^2$  at 298 K and  $0.054 \text{ F/}$

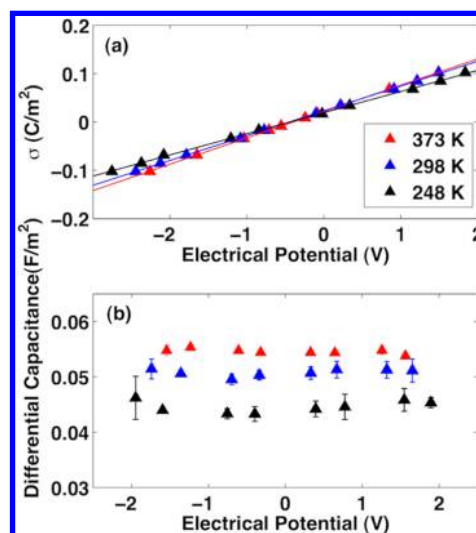


**Figure 3.** (a) Surface charge density as a function of electrical potential drop for the binary mixture at 248, 298, and 373 K. (b) The differential capacitance as a function of electrical potential for the binary mixture at 248, 298, and 373 K.

$\text{m}^2$  at 373 K). The differential capacitance for the binary mixtures at 248, 298, and 373 K are shown in Figure 3b, which reveals the same trend in temperature dependence.

The classical Gouy–Chapman theory predicts that the electrical capacitance decreases as temperature increases (referred to as negative temperature dependence).<sup>27</sup> However, a series of experiments using RTILs as electrolytes obtain the reverse trend.<sup>13–16</sup> High temperature molten salts were found to possess the positive temperature dependence of differential capacitance as well.<sup>22,23</sup> Kornyshev has pointed out that the Gouy–Chapman model is not appropriate for highly condensed ionic liquids.<sup>33</sup> Computational studies using MD simulation of RTILs electrolytes near planar graphite surfaces exhibit negative temperature dependence.<sup>17</sup> By contrast, MSA-MC theory discloses that at a low temperature range, the differential capacitance increases with temperature (positive temperature dependence), going through a point of maximum, beyond which the differential capacitance decreases with further temperature increase.<sup>18,27</sup> Even though positive temperature dependence was observed in several experiments using RTILs electrolytes, our results show the first observation of positive temperature dependence in MD simulations. To date, an acceptable explanation for this trend has not been proposed. Studies by Boda et al.<sup>21,34</sup> confirm that the positive temperature-dependent differential capacitance is more than a simple density effect, being related to the ionic pairs association, whereas such ion association increases as temperature decreases. A possible interpretation for this phenomenon is that fast dissociation of ions at high temperature results in a thinner EDL thickness, hence increasing the differential capacitance.<sup>35</sup>

To illustrate the influence of temperature on the EDL thickness, Figure 4 shows the number density profile for counterions near a positively (Figure 4a) and a negatively (Figure 4b) charged OLC electrode. Previous investigations demonstrated that at charged surfaces, the EDL structure is dominated by the counterions rather than co-ions due to strong electrostatic attraction.<sup>28</sup> Due to the overscreening of counterions near charged electrodes, alternating layers of counterions and co-ions form near the electrode to balance its net charge.



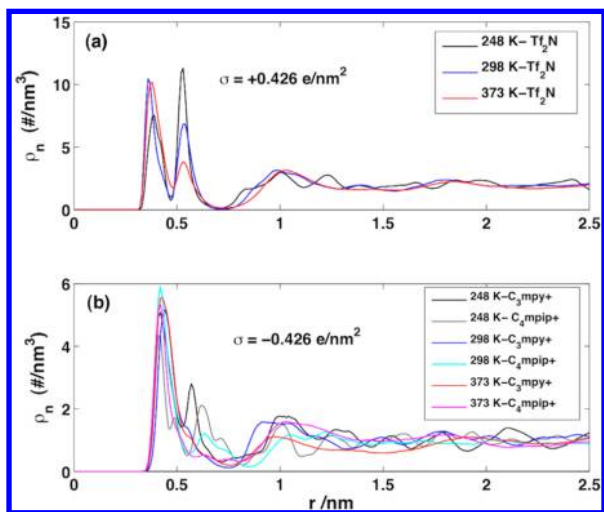


**Figure 4.** Number density profile for the binary mixture at (a) positively charged and (b) negatively charged OLC electrode at 248, 298, and 373 K.

Far from the electrode, there is no such layering formation owing to the weak electrostatic interaction between the electrode and ions.<sup>36</sup> From Figure 4, the second layer of EDL becomes more evident as temperature decreases from 373 to 248 K, suggesting that the EDL thickness increases as temperature decreases.

To quantify the EDL thickness, the effective thickness  $d_{\text{eff}}$  is introduced, which is calculated using the formula derived from ref 36:

$$d_{\text{eff}} = \frac{\int_R^r s^2(s-R)\rho_{\text{counter-ions}}^n(s)ds}{\int_R^r s^2\rho_{\text{counter-ions}}^n(s)ds}$$

$s$  is the distance between electrode surface and center of mass of ions, and  $\rho_{\text{counter-ions}}^n(s)$  is the number density profile of counterions.

$d_{\text{eff}}$  for binary mixture at 248, 273, 298, 323, and 373 K was calculated and shown in Figure 5a. Due to the near-flat differential capacitance as a function of applied potential, herein,  $d_{\text{eff}}$  is only shown at the potential of  $\sim 1.5$  V.

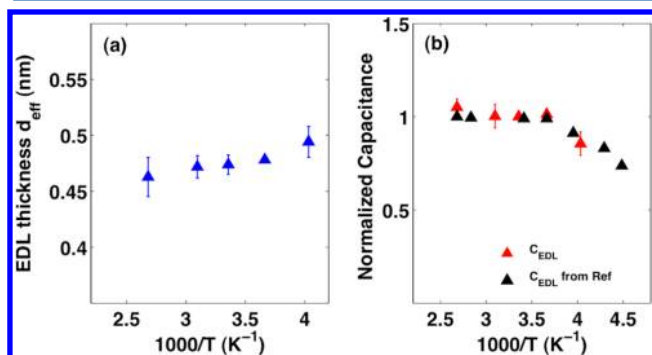


**Figure 5.** (a) EDL thickness ( $d_{\text{eff}}$ ) as a function of temperature (b) and normalized capacitance ( $C_{\text{EDL}}/C_{\text{EDL},298\text{K}}$ ) for the binary mixture near OLC in comparison with normalized capacitance ( $C_{\text{EDL}}/C_{\text{EDL},293\text{K}}$ ) taken from ref 8 as a function of temperature. The capacitances of varying temperatures at  $\sigma = 0.426$  e/nm<sup>2</sup> were chosen due to the near-flat curve of capacitance versus electrical potential.

In OLC-based supercapacitors, the capacitance can be simplified as<sup>37</sup>

$$C_{\text{EDL}} = \epsilon \left( \frac{1}{R} + \frac{1}{d_{\text{eff}}} \right)$$

where  $\epsilon$  is the dielectric constant of the EDL,  $R$  is the radius of the OLC ( $C_{720}$  herein), and  $d_{\text{eff}}$  is the thickness of the EDL structure. This formula reveals that at fixed temperature, the capacitance will increase as the size/radius of OLC decreases, which has been demonstrated in ref 12. The effective thickness  $d_{\text{eff}}$  was found to increase with decreasing temperature, as shown in Figure 5a, demonstrating the positive temperature dependence. Currently, it is still difficult to experimentally measure the interfacial dielectric constant, although its temperature-dependence and effects on the EDL cannot be completely excluded. However, as shown in Figure 5b, the positive temperature-dependent normalized capacitance for the binary mixture as a function of temperature, which is in good agreement with experimental results,<sup>8</sup> despite different RTILs being studied. Furthermore, when the temperature was lowered from 373 to 248 K, less than 20% of the differential capacitance was lost, showing that OLC-RTILs supercapacitors are suitable for low temperature use.

Although previous experimental work related the positive temperature dependence to the EDL thickness, the experimental or theoretical verification was pending. The present computational study demonstrates that the origin of the positive temperature dependence is correlated to the thinning of the EDL with increasing temperatures. Thus, these results may allow for the future design and improvement of low-temperature operated supercapacitors and electrolytes without diminishing their capacitive performance.

In summary, this study demonstrated that the binary mixture of RTILs outperformed neat RTILs as supercapacitor electrolytes with widened operation temperature, higher conductivity, and a near-flat differential capacitance as a function of electric potential. The positive temperature dependence of the differential capacitance dominated by the EDL thickness provides a theoretical model for interpreting the experimentally observed positive temperature dependence.

## ■ ASSOCIATED CONTENT

### ● Supporting Information

Methodology details and supplementary figures are all given in the Supporting Information. This material is available free of charge via the Internet <http://pubs.acs.org>.

## ■ AUTHOR INFORMATION

### Corresponding Author

\*E-mail: peter.cummings@vanderbilt.edu; Tel: 615-322-8129; Fax: 615-343-7951.

### Notes

The authors declare no competing financial interest.

## ■ ACKNOWLEDGMENTS

This work was supported as part of the Fluid Interface Reactions, Structures, and Transport (FIRST) Center, an Energy Frontier Research Center funded by the U.S. Department of Energy, Office of Science, Office of Basic Energy Sciences. S.L. gratefully acknowledges Dr. Oleg Borodin for graciously providing the APPLE&P force field parameters used in this work. Computations were performed on the Oak

Ridge National Laboratory FIRST-funded cluster and at the National Energy Research Scientific Computing Center, which is supported by the Office of Science of the U.S. Department of Energy under Contract No. DE-AC02-05CH11231.

## REFERENCES

- (1) Inagaki, M.; Konno, H.; Tanaiki, O. Carbon Materials for Electrochemical Capacitors. *J. Power Sources* **2010**, *195*, 7880–7903.
- (2) Liu, C. G.; Yu, Z. N.; Neff, D.; Zhamu, A.; Jang, B. Z. Graphene-Based Supercapacitor with an Ultrahigh Energy Density. *Nano Lett.* **2010**, *10*, 4863–4868.
- (3) Conway, B. E. *Electrochemical Supercapacitors: Scientific Fundamentals and Technological Applications*; Kluwer Academic/Plenum: New York/London, 1999.
- (4) Cheng, Q.; Tang, J.; Ma, J.; Zhang, H.; Shinya, N.; Qin, L. C. Graphene and Carbon Nanotube Composite Electrodes for Supercapacitors with Ultra-high Energy Density. *Phys. Chem. Chem. Phys.* **2011**, *13*, 17615–17624.
- (5) Kunze, M.; Jeong, S.; Paillard, E.; Winter, M.; Passerini, S. Melting Behavior of Pyrrolidinium-Based Ionic Liquids and Their Binary Mixtures. *J. Phys. Chem. C* **2010**, *114*, 12364–12369.
- (6) Egashira, M.; Kanetomo, A.; Yoshimoto, N.; Morita, M. Electrode Properties in Mixed Imidazolium Ionic Liquid Electrolytes. *Electrochemistry* **2010**, *78*, 370–374.
- (7) Zistler, M.; Wachter, P.; Schreiner, C.; Fleischmann, M.; Gerhard, D.; Wasserscheid, P.; Hinsch, A.; Goresa, H. J. Temperature Dependent Impedance Analysis of Binary Ionic Liquid Electrolytes for Dye-Sensitized Solar Cells. *J. Electrochem. Soc.* **2007**, *154*, B925–B930.
- (8) Lin, R. Y.; Taberna, P. L.; Fantini, S.; Presser, V.; Perez, C. R.; Malbosc, F.; Rupesinghe, N. L.; Teo, K. B. K.; Gogotsi, Y.; Simon, P. Capacitive Energy Storage from –50 to 100 °C Using an Ionic Liquid Electrolyte. *J. Phys. Chem. Lett.* **2011**, *2*, 2396–2401.
- (9) Portet, C.; Yushin, G.; Gogotsi, Y. Electrochemical Performance of Carbon Onions, Nanodiamonds, Carbon Black and Multiwalled Nanotubes in Electrical Double Layer Capacitors. *Carbon* **2007**, *45*, 2511–2518.
- (10) McDonough, J. K.; Frolov, A. I.; Presser, V.; Niu, J.; Miller, C. H.; Ubieto, T.; Fedorov, M. V.; Gogotsi, Y. Influence of the Structure of Carbon Onions on Their Electrochemical Performance in Supercapacitor Electrodes. *Carbon* **2012**, 3298–3309.
- (11) Pech, D.; Brunet, M.; Durou, H.; Huang, P. H.; Mochalin, V.; Gogotsi, Y.; Taberna, P. L.; Simon, P. Ultrahigh-Power Micrometre-Sized Supercapacitors Based on Onion-like Carbon. *Nat. Nanotechnol.* **2010**, *5*, 651–654.
- (12) Feng, G.; Jiang, D.; Cummings, P. T. Curvature Effect on the Capacitance of Electric Double Layers at Ionic Liquid/Onion-like Carbon Interfaces. *J. Chem. Theory Comput.* **2012**, 1058–1063.
- (13) Costa, R.; Pereira, C. M.; Silva, F. Double Layer in Room Temperature Ionic Liquids: Influence of Temperature and Ionic Size on the Differential Capacitance and Electrocapillary Curves. *Phys. Chem. Chem. Phys.* **2010**, *12*, 11125–11132.
- (14) Lockett, V.; Sedev, R.; Ralston, J.; Horne, M.; Rodopoulos, T. Differential Capacitance of the Electrical Double Layer in Imidazolium-Based Ionic Liquids: Influence of Potential, Cation Size, and Temperature. *J. Phys. Chem. C* **2008**, *112*, 7486–7495.
- (15) Silva, F.; Gornes, C.; Figueiredo, M.; Costa, R.; Martins, A.; Pereira, C. M. The Electrical Double Layer at the [BMIM][PF<sub>6</sub>] Ionic Liquid/Electrode Interface - Effect of Temperature on the Differential Capacitance. *J. Electroanal. Chem.* **2008**, *622*, 153–160.
- (16) Fletcher, S. I.; Sillars, F. B.; Carter, R. C.; Cruden, A. J.; Mirzaeian, M.; Hudson, N. E.; Parkinson, J. A.; Hall, P. J. The Effects of Temperature on the Performance of Electrochemical Double Layer Capacitors. *J. Power Sources* **2010**, *195*, 7484–7488.
- (17) Vatamanu, J.; Borodin, O.; Smith, G. D. Molecular Insights into the Potential and Temperature Dependences of the Differential Capacitance of a Room-Temperature Ionic Liquid at Graphite Electrodes. *J. Am. Chem. Soc.* **2010**, *132*, 14825–14833.
- (18) Boda, D.; Henderson, D.; Chan, K. Y. Monte Carlo Study of the Capacitance of the Double Layer in a Model Molten Salt. *J. Chem. Phys.* **1999**, *110*, 5346–5350.
- (19) Boda, D.; Henderson, D. The Capacitance of the Solvent Primitive Model Double Layer at Low Effective Temperatures. *J. Chem. Phys.* **2000**, *112*, 8934–8938.
- (20) Reszko-Zygmunt, J.; Sokolowski, S.; Henderson, D.; Boda, D. Temperature Dependence of the Double Layer Capacitance for the Restricted Primitive Model of an Electrolyte Solution from a Density Functional Approach. *J. Chem. Phys.* **2005**, *122*, 084504.
- (21) Boda, D.; Henderson, D.; Chan, K. Y.; Wasan, D. T. Low Temperature Anomalies in the Properties of the Electrochemical Interface. *Chem. Phys. Lett.* **1999**, *308*, 473–478.
- (22) Ukshe, E. A.; Bukun, N. G.; Leikis, D. I.; Frumkin, A. N. Investigation of the Electric Double Layer in Salt Melts. *Electrochim. Acta* **1964**, *9*, 431–439.
- (23) Bukun, N. G. T.; N. S.; Ukshe, E. A. Double Layer Capacity on Molybdenum in Fused Salts. *Elektrokhimiya* **1970**, *6*, 1215–1218.
- (24) Alam, M. T.; Islam, M. M.; Okajima, T.; Ohsaka, T. Measurements of Differential Capacitance at Mercury/Room-Temperature Ionic Liquids Interfaces. *J. Phys. Chem. C* **2007**, *111*, 18326–18333.
- (25) Kiszka, A. The Capacitance of the Diffuse Layer of Electric Double Layer of Electrodes in Molten Salts. *Electrochim. Acta* **2006**, *51*, 2315–2321.
- (26) Loth, M. S.; Skinner, B.; Shklovskii, B. I. Anomalous Large Capacitance of an Ionic Liquid Described by the Restricted Primitive Model. *Phys. Rev. E* **2010**, *82*, 056102.
- (27) Holovko, M.; Kapko, V.; Henderson, D.; Boda, D. On the Influence of Ionic Association on the Capacitance of an Electrical Double Layer. *Chem. Phys. Lett.* **2001**, *341*, 363–368.
- (28) Feng, G.; Zhang, J. S.; Qiao, R. Microstructure and Capacitance of the Electrical Double Layers at the Interface of Ionic Liquids and Planar Electrodes. *J. Phys. Chem. C* **2009**, *113*, 4549–4559.
- (29) Vatamanu, J.; Borodin, O.; Smith, G. D. Molecular Simulations of the Electric Double Layer Structure, Differential Capacitance, and Charging Kinetics for *N*-Methyl-*N*-propylpyrrolidinium Bis-(fluorosulfonyl)imide at Graphite Electrodes. *J. Phys. Chem. B* **2011**, *115*, 3073–3084.
- (30) Salminen, J.; Papaiconomou, N.; Kumara, R. A.; Lee, J. M.; Kerr, J.; Newman, J.; Prausnitz, J. M. Physicochemical Properties and Toxicities of Hydrophobic Piperidinium and Pyrrolidinium Ionic Liquids. *Fluid Phase Equilib.* **2007**, *261*, 421–426.
- (31) Triolo, A.; Russina, O.; Fazio, B.; Appetecchi, G. B.; Carewska, M.; Passerini, S. Nanoscale Organization in Piperidinium-Based Room Temperature Ionic Liquids. *J. Chem. Phys.* **2009**, *130*, 164521.
- (32) Si, X. J.; Li, S.; Wang, Y. L.; Ye, S. H.; Yan, T. Y. Effects of Specific Adsorption on the Differential Capacitance of Imidazolium-Based Ionic Liquid Electrolytes. *ChemPhysChem* **2012**, *13*, 1671–1676.
- (33) Kornyshev, A. A. Double-Layer in Ionic Liquids: Paradigm Change? *J. Phys. Chem. B* **2007**, *111*, 5545–5557.
- (34) Holovko, M.; Kapko, V.; Henderson, D.; Boda, D. On the Influence of Ionic Association on the Capacitance of an Electrical Double Layer. *Chem. Phys. Lett.* **2001**, *341*, 363–368.
- (35) Lockett, V.; Horne, M.; Sedev, R.; Rodopoulos, T.; Ralston, J. Differential Capacitance of the Double Layer at the Electrode/Ionic Liquids Interface. *Phys. Chem. Chem. Phys.* **2010**, *12*, 12499–12512.
- (36) Feng, G.; Huang, J. S.; Sumpter, B. G.; Meunier, V.; Qiao, R. A. “Counter-Charge Layer in Generalized Solvents” Framework for Electrical Double Layers in Neat and Hybrid Ionic Liquid Electrolytes. *Phys. Chem. Chem. Phys.* **2011**, *13*, 14723–14734.
- (37) Huang, J. S.; Sumpter, B. G.; Meunier, V.; Yushin, G.; Portet, C.; Gogotsi, Y. Curvature Effects in Carbon Nanomaterials: Exohedral versus Endohedral Supercapacitors. *J. Mater. Res.* **2010**, *25*, 1525–1531.